Journal of Catalysis 271 (2010) 220–227

Contents lists available at ScienceDirect

Journal of Catalysis

journal homepage: www.elsevier.com/locate/jcat

Preparation of different basic Si–MCM-41 catalysts and application in the Knoevenagel and Claisen–Schmidt condensation reactions

Leandro Martins [a,b], Wolfgang Hölderich [b], Peter Hammer [c], Dilson Cardoso [a,*]

[a] Chemical Engineering Department, Federal University of São Carlos, Rodovia Washington Luís 235, 13565-905, São Carlos, Brazil
[b] Department of Chemical Technology and Heterogeneous Catalysis, RWTH-Aachen, Worringerweg 1, 52074 Aachen, Germany
[c] Instituto de Química, UNESP – Univ Estadual Paulista, 14801-970 Araraquara, SP, Brazil

ARTICLE INFO

Article history:
Received 3 November 2009
Revised 8 January 2010
Accepted 15 January 2010
Available online 18 February 2010

Keywords:
Si–MCM-41
Basic catalysis
Knoevenagel condensation
Hybrid organic–inorganic mesoporous materials

ABSTRACT

In the present work, the basicity of three different Si–MCM-41 mesoporous materials, namely, (1) as-synthesized Si–MCM-41, (2) Si–MCM-41 modified by dispersing cesium oxide (Cs_2O) and (3) Si–MCM-41 with anchored aminopropylsilyl group was compared for the first time. The fact that Knoevenagel and Claisen–Schmidt condensations stand out to be important in carbon–carbon bond formation as well as in the preparation of fine chemicals and intermediates, led them to be used as model reactions for the purpose of evaluating the catalytic performance. The activity of the modified samples was compared with that of the as-synthesized material [CTA^+]–Si–MCM-41 (where CTA^+ stands for the structure directing agent). This catalyst presented the highest catalytic activity compared to that of Si–MCM-41 modified with Cs_2O or aminopropylsilyl group. This is of extreme high advantage, because it can be used as-synthesized without further modification. Furthermore, structural properties of the Si–MCM-41 samples were determined based on X-ray diffraction measurements (XRD), nitrogen adsorption/desorption isotherms, ^{29}Si nuclear magnetic resonance (MAS NMR) and X-ray photoelectron spectroscopy (XPS).

1. Introduction

There is a vast interest in the use of heterogeneous catalytic processes as a substitute for homogeneous catalysis, which suffers from several environmental drawbacks. Nevertheless, in basic catalysis, the use of homogeneous media is currently more common in comparison with the eco-friendly heterogeneous media [1,2]. Recently, heterogenization of homogeneous catalysts has become an important strategy for the preparation of supported catalysts which retain the active catalytic sites of the homogeneous analogue and provide at the same time advantages of easy separation and recycling as well as reusability of the catalysts [3,4].

One well-known and widely mentioned material in the last years is the siliceous mesoporous molecular sieve from Mobil, denoted with number 41 (Si–MCM-41) [5]. Its highly ordered pore systems and extremely high surface area of up to 1200 m^2/g have drawn immense attention. The presence of groups able to be functionalized (*i.e.* silanol groups) makes them useful as support for organic compounds and metal oxides on which very high dispersion of the active phase can be achieved [3,6]. Additionally, these materials present potential application in processes dealing with large molecules as in fine chemistry and pharmaceutical production, without the stereo spatial limitations in the case of microporous molecular sieves.

Although MCM-41 was discovered in 1992, many properties have already been explored, and the commercial application of some of them is likely underway. Surprisingly, a novel property of this molecular sieve was found recently: as-synthesized Si–MCM-41, denoted [CTA^+]–Si–MCM-41 (CTA stands for cetyltrimethylammonium cation), showing interesting and remarkable basic properties. This attractive catalyst has already been tested in three different reactions: Knoevenagel condensation [7–11], Michael addition [12] and cycloaddition reaction of CO_2 with epoxides [13].

The basic properties of [CTA^+]–Si–MCM-41 are resultant of the presence of siloxy anions ($\equiv SiO^-$), which exist in combination with the cationic surfactant [8,9]. The existence of the ionic pair $\equiv SiO^- CTA^+$ has been demonstrated by various authors [8,9,14,15]. In fact, during the synthesis of the [CTA^+]–Si–MCM-41 material, the specific arrangement of the cationic organic molecules supports the ordering of the structure at the micelle–silicate interface [16], hence generating the siloxy anions. Because the MCM-41 catalyst channels are filled with the ionic surfactant, the high activity in the investigated reactions is attributed to basic sites present at the pore-mouth. The [CTA^+]–Si–MCM-41 possesses a surface area of only 1 m^2/g, and therefore the basic sites present inside the channels are inaccessible for the reactants [9]. This catalyst shows high catalytic activity even at low temperatures and has in

* Corresponding author. Fax: +55 16 3351 8266.
E-mail address: dilson@ufscar.br (D. Cardoso).

0021-9517/$ - see front matter © 2010 Elsevier Inc. All rights reserved.
doi:10.1016/j.jcat.2010.01.015

addition an extra great advantage, because it can be used as-synthesized, without further modification.

The catalytic stability of the [CTA$^+$]–Si–MCM-41 molecular sieve was previously tested in toluene media [9,10]. After each reaction procedure, the catalyst was separated by centrifugation, vacuum dried and reused without any further treatment [10]. Under these conditions, the catalyst showed only minor deactivation accompanied with a small loss of the CTA$^+$ surfactant. This leaching process resulting from CTA cations that are weakly connected to the micelles contributed to lower its catalytic activity. Apart from that, no further significant activity loss was observed after the fourth use. The stability of the remaining surfactant cations inside the pores can be explained by the strong interaction between the non-polar molecule tails of the surfactants in the micelle [17,18].

In general, the basicity in calcined Si–MCM-41 molecular sieve is achieved by functionalizing its surface with compounds containing terminal amines [3,6]. The material is functionalized by anchoring organic bases at the silanol groups, thereby forming a covalent bond. Unfortunately, these organic–inorganic hybrid materials are less basic than the corresponding free organic amine molecule. This fact has already been explained as involving the interaction of the amine function with residual silanol groups [19]. Prior to functionalizing, the cationic surfactants present in the pores have to be removed in the first place in order to make the pores free and to generate the silanol groups, usually carried out by calcination under airflow. Here, special care has to be taken, because high local temperature can lead to the condensation of neighboring silanol groups as well as the reduction in their number, thus limiting the number of organic molecules to be anchored [3].

Another method of obtaining basic Si–MCM-41 can be achieved by dispersing alkali metal oxides [20,21]. However, due to the pH of the impregnating solution, the Si–MCM-41 structure can be somewhat damaged [20]. It is well known that Si–O bonds, present in these materials, undergo hydrolysis even in slightly elevated pH (≅8.5) environments. Because Si–MCM-41 has high surface area and tiny walls, the hydrolysis of these bonds takes place easily. Cesium acetate is usually used for the impregnation of calcined Si–MCM-41, followed by heating to generate the basic Cs_2O centers [21]. Alkali metals and metal oxides are among the strongest bases known. Nevertheless, these oxides have a very low surface area, which limits their application as efficient catalysts. For this reason, by supporting these oxides on higher surface area carriers (*i.e.* siliceous mesoporous materials), it is expected to obtain materials exhibiting strong basicity and a high number of well-dispersed single basic sites. Since cesium oxide creates stronger basic centers than other alkali metals, researchers have focused their attention on supported cesium catalysts.

Many basic materials have been tested as catalysts in condensation reactions. Most of them involve much simpler preparation procedures such as hydrotalcites, zeolites or even very simple and efficient catalysts with a high surface area of MgO [22]. Additionally, these catalysts can be reused without great loss of activity. While literature data show that other catalysts perform quite well in the process involving the synthesis of fine chemicals, the nature as well as the scope of this present work has been made to focus solely and objectively on Si–MCM-41.

The aim of the present research is to compare the catalytic properties of a series of Si–MCM-41 molecular sieves, containing different basic sites including: (1) as-synthesized [CTA$^+$]–Si–MCM-41, (2) functionalized Si–MCM-41, enclosing aminopropyl group and (3) cesium containing Si–MCM-41. The structural properties of the samples were characterized by X-ray powder diffraction (XRD), nitrogen adsorption/desorption isotherms (BET surface area and BJH pore size distribution), ^{29}Si MAS NMR (nuclear magnetic resonance) and X-ray photoelectron spectroscopy (XPS). These materials were tested in the Knoevenagel condensation as a model reaction and in the more demanding Claisen–Schmidt reaction.

2. Experimental

2.1. Synthesis of Si–MCM-41 catalysts

The mesoporous material [CTA$^+$]–Si–MCM-41 (denoted as Catalyst A, step I in Scheme 1) was synthesized using tetraethoxysilane (TEOS), aqueous ammonia (NH_4OH), absolute ethanol (EtOH) as co-solvent and the organic template $C_{16}H_{33}N(CH_3)_3Br$ (CTA$^+$Br$^-$, Scheme 1) [10]. The molar composition of the reaction medium

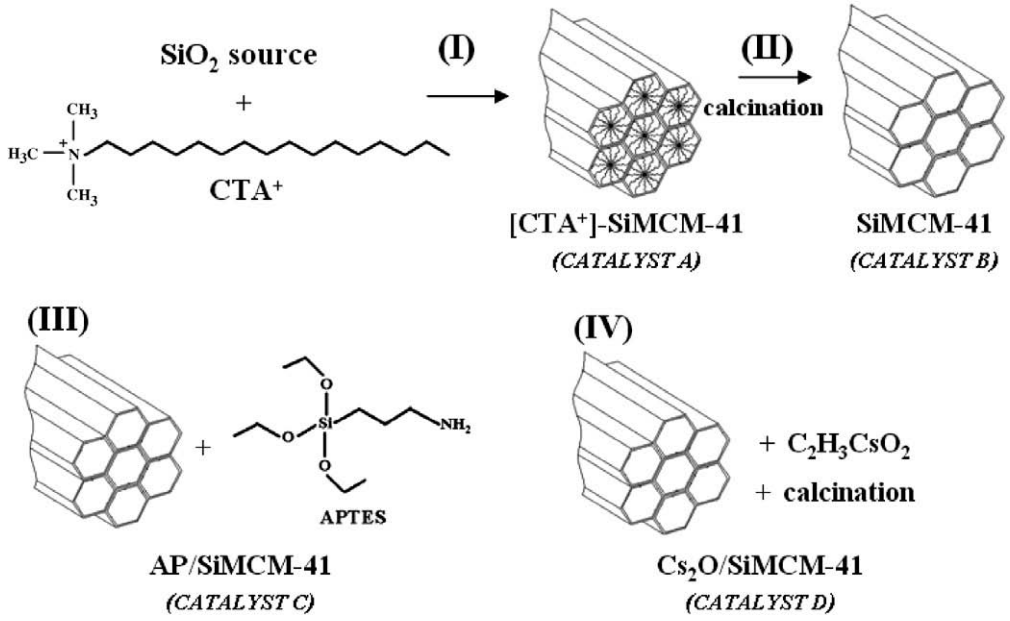

Scheme 1. Preparation of the catalysts: (I) [CTA$^+$]–Si–MCM-41 synthesis; (II) CTA$^+$ cation removal by calcination; (III) functionalization of Si–MCM-41 (Catalyst B) by treating the calcined material with APTES and (IV) dispersion of $C_2H_3CsO_2$ on Si–MCM-41 (Catalyst B) followed by calcination.

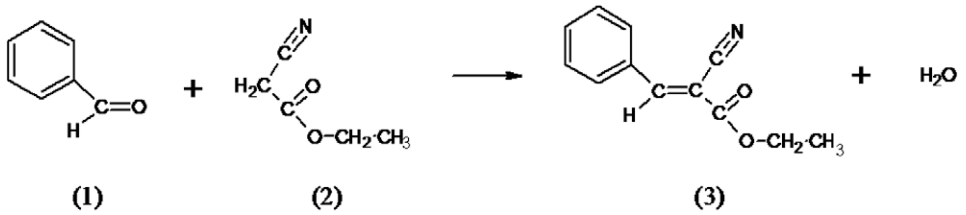

Scheme 2. Knoevenagel condensation reaction between benzaldehyde and ethyl cyanoacetate.

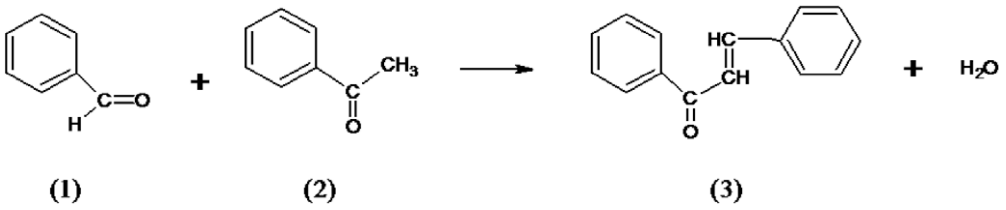

Scheme 3. Claisen–Schmidt condensation reaction between benzaldehyde and acetophenone.

was 1.0 TEOS:0.3 CTABr:11 NH_3:144 H_2O:28 EtOH, which has shown to lead to high mesoporous phase ordering degree [10]. A typical [CTA^+]–Si–MCM-41 preparation procedure is described as follows: 26.0 g of CTA^+Br^- (ABCR, 98 wt.%) was dissolved in 334.0 g of deionized water; 327.4 g of aqueous ammonia (28 wt.% solution, Alfa Aesar) and 263.0 g of absolute ethanol was added to the surfactant solution. The solution was then stirred for 15 min, and afterwards 49.6 g of TEOS (Fluka, 98 wt.%) was added. After 2 h of vigorous stirring at 30 °C and filtration, the white precipitate was successively washed with plenty of distilled water and dried at 60 °C for 24 h. A total of 29.7 g of [CTA^+]–Si–MCM-41 was obtained.

With the aim of obtaining Si–MCM-41 (Catalyst B, step II in Scheme 1), a part of the [CTA^+]–Si–MCM-41 sample was calcined, under oxygen atmosphere, through a heating ramp of 1 °C/min up to 520 °C and then kept at this same temperature for 6 h.

Functionalized Si–MCM-41 (Catalyst C) was obtained by treating the calcined material with aminopropyltriethoxysilane (APTES, step III in Scheme 1). In a typical procedure, Si–MCM-41 material (4 g) was vacuum dried ($<5 \times 10^{-2}$ bar) at 150 °C for 3 h and immediately suspended in anhydrous toluene (40 g). An amount of 1.328 g (6.0 mmol) of APTES (Fluka, 96 wt.%) was added to this suspension, and the mixture was further stirred under reflux for 3 h. Toluene and the produced ethanol were distilled off under vacuum, and the obtained material was denoted as AP–Si–MCM-41 (Catalyst C, whereby AP stands for aminopropylsilyl group).

Cs_2O–Si–MCM-41 (Catalyst D, Scheme 1) was obtained by incipient wetness impregnation of calcined and dried Si–MCM-41 (4 g) using 10 mL of a 0.6 mol/L solution of cesium acetate (CsOAc, Strem Chemical 99.9 wt.%). The mixture, CsOAc and Si–MCM-41, was dried at room temperature and again calcined at 500 °C for 4 h.

2.2. Knoevenagel and Claisen–Schmidt condensation reactions in the batch reactor

The condensation reactions were performed in a 2-mL borosilicate glass reactor (GC type tapered flask, with silicon septum). The reactor was immersed in a water bath, equipped with temperature control. The condensation reactions, between benzaldehyde and ethyl cyanoacetate at 30 °C (Scheme 2, Knoevenagel) and between benzaldehyde and acetophenone at 120 °C (Scheme 3, Claisen–Schmidt), were carried out using stoichiometric amounts of the reactants (4.8 mmol), 20 mg of the catalyst (1.9 wt.%) for 3 h. The Knoevenagel reaction was also carried out in toluene as solvent using initial reactants concentration of 0.5 mol/L. Sampling was achieved first by removing the catalyst in rapid centrifugation (one minute) and then cooling the liquid product, which was further analyzed using gas chromatography (GC, Siemens RGC 202). For this purpose, a DB-1 capillary column (100 m) with a flame ionization detector was used. The carrier gas was N_2 (1.5 bar), and the analysis temperature was 230 °C (oven temperature), 220 °C (injector) and 280 °C (detector). The retention times were compared with those of authentic compounds.

2.3. Knoevenagel condensation in continuous operating plug-flow reactor

Furthermore, [CTA^+]–Si–MCM-41 catalyst activity in Knoevenagel condensation was investigated in a continuous flow reactor for 100 h. For the purpose of limiting the pressure drop through the packed bed, the catalyst was granulated. The powder was then pressed at 8 ton/cm^2 to form pellets which afterwards were crushed and sieved to 1.0–1.6 mm size. The resultant pellets (5.5 g) were transferred to a glass reactor with controlled temperature device (30 °C). A continuous flow (8 mL/h) of benzaldehyde and ethyl cyanoacetate mixture in toluene (reactants concentration of 0.5 mol/L) was used.

3. Characterization

3.1. X-ray powder diffraction

Small-angle X-ray diffraction patterns were recorded on a Siemens D-5000 diffractometer, using the powder method, in the $1 < 2\theta < 10°$ interval. Cu Kα radiation ($\lambda = 0.15405$ nm) and nickel filter were used. The distance (a_H) between pore centers of the hexagonal structure was calculated from $a_H = 2d_{100}/(3)^{1/2}$.

3.2. Surface area analysis

Nitrogen adsorption/desorption isotherms were recorded at liquid nitrogen temperature using the equipment supplied by Micromeritics (ASAP 2000). Samples were evacuated prior to measurements at 120 °C for 12 h under a vacuum of 0.01 Pa. Surface

areas were estimated from the BET equation using $P/P_o \leqslant 0.3$ [23], while the pore diameters, D_{Pore}, were calculated from the inflection point of the cumulative pore volume *versus* diameter curve obtained from the corrected form of BJH equation [24].

3.3. Elemental analysis

Carbon, hydrogen and nitrogen mass percentages were determined using the Elementar Vario EL. All analyses were carried out in duplicate.

3.4. ^{29}Si MAS NMR

^{29}Si magic-angle spinning (MAS) nuclear magnetic resonance (NMR) spectra were recorded at room temperature with a Bruker DSX 500 spectrometer, using a 4-mm rotor operating at 400 MHz. Magic-angle spinning at 5 kHz was used in all experiments. NMR experiments were performed using a 5-ms $\pi/2$ excitation pulse and 30 s of recycle delay.

3.5. XPS

The XPS measurements were carried out using a commercial spectrometer (UNI-SPECS UHV). The Mg Kα line was used ($h\nu$ = 1253.6 eV), and the pass energy of the analyzer was set to 10 eV. The inelastic background of the C 1s, O 1s, N 1s and Si 2p core-level spectra was subtracted using Shirleý's method. The binding energies of the spectra were corrected using the hydrocarbon component of adventitious carbon fixed at 285.0 eV. The composition of the surface layer was determined from the ratios of the relative peak areas corrected by sensitivity factors for the corresponding elements. The spectra were fitted using multiple Voigt profiles without placing constraints. The width at half maximum (FWHM) varied between 1.5 and 2.2 eV, and the accuracy of the peak positions was ±0.1 eV.

4. Results and discussion

4.1. Characterization of Si–MCM-41 samples

The small-angle X-ray diffraction pattern of the as-synthesized [CTA$^+$]–Si–MCM-41 sample (catalyst A) shows four well-resolved peaks (Fig. 1, curve 1) that can be indexed as (1 0 0), (1 1 0), (2 0 0) and (2 1 0) reflections associated with the hexagonal symmetry [5]. No diffraction peak was observed in the region of higher angles between 10° and 40° (not shown), indicating the absence of other silicate phases. The distance a_H between the pore centers contracted from 4.74 to 3.89 nm (as can be seen in Table 1) when the sample was calcined, as expected when CTA cations are removed, and the adjacent silanol groups condensed. As a result, the BET specific area increased from 9 to 1272 m^2/g. Upon aminopropylsilyl immobilization in the calcined Si–MCM-41 sample, no significant change was observed in the XRD pattern (Fig. 1, curve 3). In contrast, the X-ray powder pattern of cesium–MCM-41 was strongly affected by the impregnation of the host material and subsequent calcination, which thereby led to an increase in the background intensity. This effect can be partially attributed to the strong X-ray absorption of cesium atoms, as can be seen in the Si–MCM-41 sample physically mixed with CsOAc (Fig. 1, curve 4). However, for the calcined sample (Cs_2O–Si–MCM-41), the X-Ray diffraction pattern (Fig. 1, curve 5) and nitrogen sorption isotherm (Fig. 2, curve 4 and Table 1) indicate the transformation of the silicate hexagonal arrangement into amorphous phase [5]. This collapse of the pore system may be caused by the cesium oxide together with the steam generated by the combustion of the acetate precursor during calcination. Here is worthy to be mentioned a stable system of cesium and lanthanum oxide supported on Si–MCM-41 previously developed by Kloetstra et al. [25]. These materials possess small, intraporous, thermally stable $CsLaO_x$ clusters having a mild basicity. The presence of $CsLaO_x$ helped in maintaining the stability of the mesoporous framework.

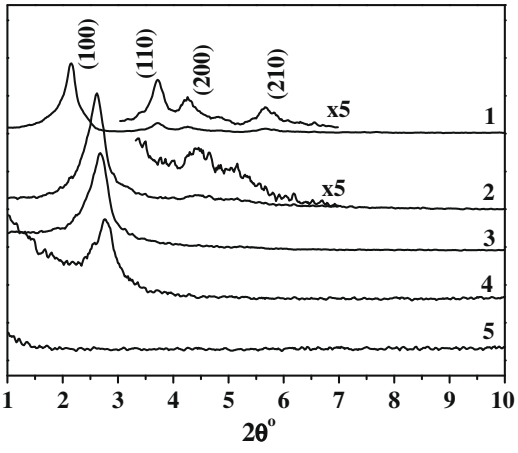

Fig. 1. X-ray diffraction patterns of MCM-41 molecular sieves (1) [CTA$^+$]–Si–MCM-41, (2) Si–MCM-41, (3) AP–Si–MCM-41, (4) CsOAc–Si–MCM-41 not calcined and (5) Cs_2O–Si–MCM-41 calcined.

Table 2 presents the chemical composition of the MCM-41 samples. Elemental C, H and N analysis of [CTA$^+$]–Si–MCM-41 and AP–Si–MCM-41 samples showed a *C*/*N* ratio close to 19 and 3, corresponding to the chemical composition of CTA and AP, respectively. The samples AP–Si–MCM-41 and Cs_2O–Si–MCM-41 were prepared in order to obtain comparable amounts of the guest material (GM), *i.e.* GM/Si molar ratio of 0.09 (GM = AP or Cs). Sample [CTA$^+$]–Si–MCM-41 had a CTA/Si molar ratio of 0.18; however, this value does not represent a real amount of GM effectively in contact with the reactants during catalysis, because most of the CTA cationic surfactants are occluded inside the mesopores. This means that the reactants cannot reach active sites located in the interior of the pores but can only get to those at the pore-mouth.

Nitrogen sorption isotherms of the samples containing different guest materials are presented in Fig. 2. Two major trends related to the successive post-treatment observed are highlighted as follows: (1) the variation of the total pore volume and (2) a shift of the capillary condensation step. The calcined Si–MCM-41 material (Fig. 2A, curve 1) exhibits a type IV isotherm typical of mesoporous materials. A similar isotherm profile was observed after the immobilization of the aminopropylsilyl group (curve 2), indicating the preservation of the mesoporous structure. However, in this sample, the nitrogen uptake decreased (Table 1), suggesting the presence of bulky material inside the silica channels. The decrease of the average pore diameter (from 2.5 nm to 1.8 nm, Table 1) is a clear indication of the successful anchoring of the aminopropylsilyl group inside the Si–MCM-41 porous system.

Table 1
Structural parameters of Si–MCM-41 molecular sieves containing different guest materials.

Sample	BET surface area (m^2/g)	V_p (cm^3/g)	a_H (nm)	D_{Pore} (nm)
[CTA$^+$]–Si–MCM-41	9	0.02	4.74	–
Si–MCM-41	1272	0.68	3.89	2.5
AP–Si–MCM-41	537	0.30	3.83	1.8
CsOAc–Si–MCM-41	144	0.23	3.96	2.3
Cs_2O–Si–MCM-41	25	0.05	–	2.3 (1.5–5.6)

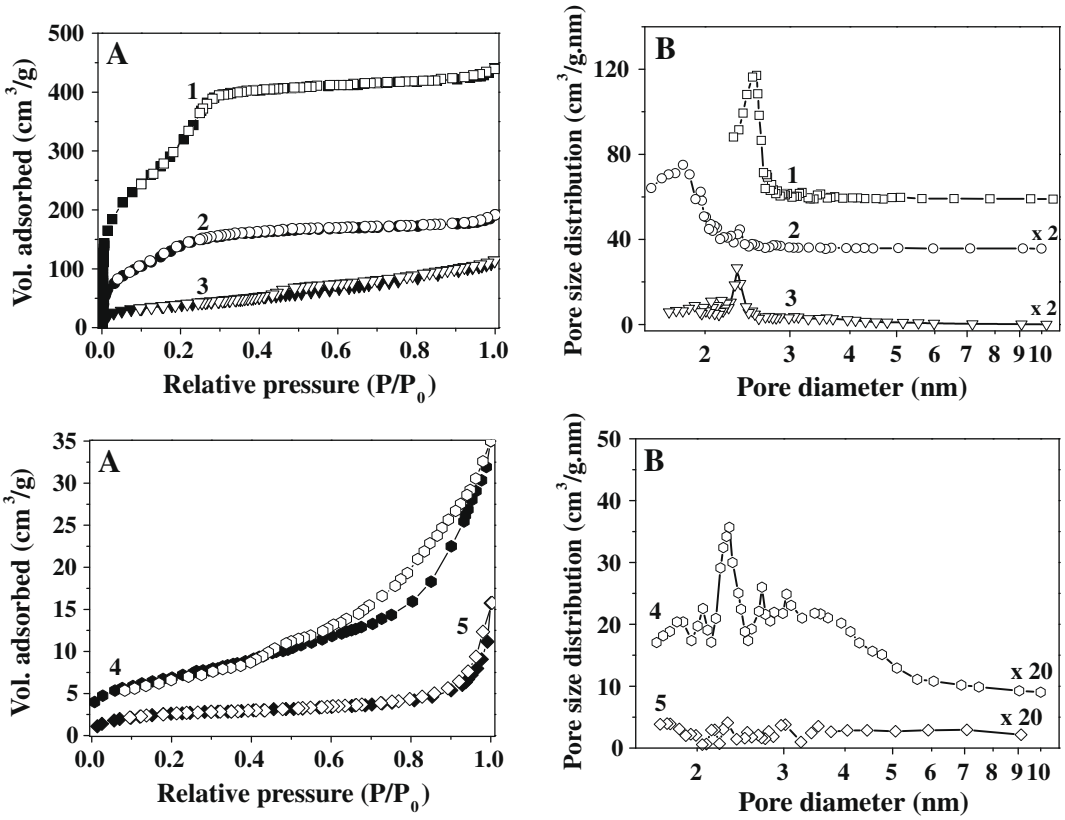

Fig. 2. (A) Nitrogen physisorption isotherms and (B) BJH pore diameter distribution of MCM-41 molecular sieves: (1) Si–MCM-41, (2) AP–Si–MCM-41 and (3) CsOAc–Si–MCM-41 not calcined, (4) Cs_2O–Si–MCM-41 calcined and (5) [CTA^+]–Si–MCM-41. Filled and empty symbols stand for adsorption and desorption, respectively.

Table 2
Chemical composition of Si–MCM-41 catalysts containing different guest materials.

Sample	Mass percentage			*C*/*N* (molar ratio)	GM[a]/Si (molar ratio)	GM (wt.%)
	%N	%C	%H			
[CTA^+]–Si–MCM-41	1.93	30.87	6.67	18.6	0.18	38.6
Si–MCM-41	–	–	–	–	–	–
AP–Si–MCM-41	1.91	5.22	3.31	3.2	0.09	8.2
CsOAc–Si–MCM-41	n.d.	n.d.	n.d.	n.d.	0.09	22.2
Cs_2O–Si–MCM-41	–	–	–	–	0.09	17.3

[a] Guest material, *i.e.* CTA^+, AP or Cs.

Upon the impregnation with cesium, the Si–MCM-41 material exhibited a considerable change in its textural properties, as shown in Fig. 2B (curve 3). After the incipient wetness impregnation, it was observed that there was a decrease in the mean pore diameter, the pore volume, as well as in the specific surface area (Table 1). A broader distribution of mesopores is shown in Fig. 2B (curve 4, D_{Pore} between 1.5 and 5.6 nm with a maximum at 2.3 nm), indicating the disruption of the regular network. The occluded [CTA^+]–Si–MCM-41 catalyst showed a very low surface area of 9 m^2/g (Table 1) related to the external surface of the siliceous material as no pores were found for this sample (Fig. 2B, curve 5).

The ^{29}Si MAS NMR spectra (hydrogen–silicon cross polarization) for Si–MCM-41 catalysts containing different guest materials are shown in Fig. 3. The technique was used to analyze the changes in the chemical environment of Si–MCM-41 after the addition of guest materials and calcination. Three distinct resonance peaks at −95, −101 and −110 ppm are attributed to the Q^2, Q^3 and Q^4 silicon atoms (Q^i = $Si(OSi)_i(OH)_{4-i}$, i = 1–4), respectively, and two other peaks at −60 and −70 ppm are attributed to the T^2 and T^3 silicon atoms (T^i = $RSi(OSi)_i(OH)_{3-i}$, i = 1–3, R = aminopropyl), respectively. The signal Q^3 is most intense in sample Si–MCM-41 (curve 2). A quantitative conclusion from this result cannot be drawn; however, this result reflects the higher amount of silanol groups ≡SiOH existent in this calcined sample. The appearance of peaks T^2 and T^3 in the AP–Si–MCM-41 sample (curve 3) provides a proof that the organosiloxane precursor APTES is condensed as a part of the silica framework. No signal at −45 ppm is observed, which corresponds to the silicon atom bonded in APTES, indicating that the compound reacted completely. The intensity of Q^3 signal in AP–Si–MCM-41 is reduced after the immobilization, which is an additional proof that silanol groups were used in the grafting. Comparing samples [CTA^+]–Si–MCM-41 and Si–MCM-41 (curves 1 and 2), we found out that there was a difference between the spectra, especially for the Q^2 signal, as a consequence of the different

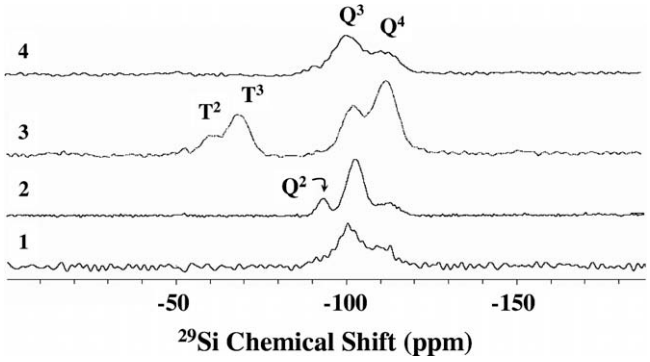

Fig. 3. ^{29}Si MAS NMR solid-state spectra (cross polarization) of different Si–MCM-41 catalysts: (1) [CTA^+]–Si–MCM-41, (2) Si–MCM-41, (3) AP–Si–MCM-41 and (4) Cs_2O–Si–MCM-41.

chemical environment of ≡SiOH and ≡SiO⁻CTA⁺ of both samples. Moreover, the spectrum of sample Cs_2O/Si–MCM-41 (curve 4) differs from that of Si–MCM-41, an outcome expected with the transformations with cesium acetate and calcination. The disappearance of signal Q^2 in sample Cs_2O/Si–MCM-41 suggests the condensation between neighbor silanol groups during calcination for the decomposition of cesium acetate.

In the spectral analysis of the XPS data, the attention was focused on O1s and C1s core-level spectra. The shift in binding energy of O1s components was investigated by XPS prior to and after calcination of [CTA⁺]–Si–MCM-41 (Fig. 4). The O1s binding energies shift significantly with the presence of CTA⁺, suggesting that the chemical form of the surface oxygen species changes according to the structural attribution shown in Table 3. The O1s binding energy corresponding to SiO_2 (Fig. 4, peak 2 and Table 3) shifts to a lower binding energy level in the presence of the CTA⁺ cations (from 532.8 to 532.3 eV), indicating that the framework oxygen basicity increases in the composite material [9]. Furthermore, the O1s spectrum of [CTA⁺]–Si–MCM-41 shows a smaller component at lower binding energy (530.2 eV), which can be attributed to siloxy anion interacting with CTA⁺ cation as ≡SiO⁻$(CH_3)_3$–⁺N–$C_{16}H_{33}$. This interaction of the hydrophilic head of the surfactant ($(CH_3)_3$–⁺N–) with siloxy anions was also detected for this component in the C1s spectrum, which shifted from 285.9 to 286.4 eV compared to the CTABr precursor.

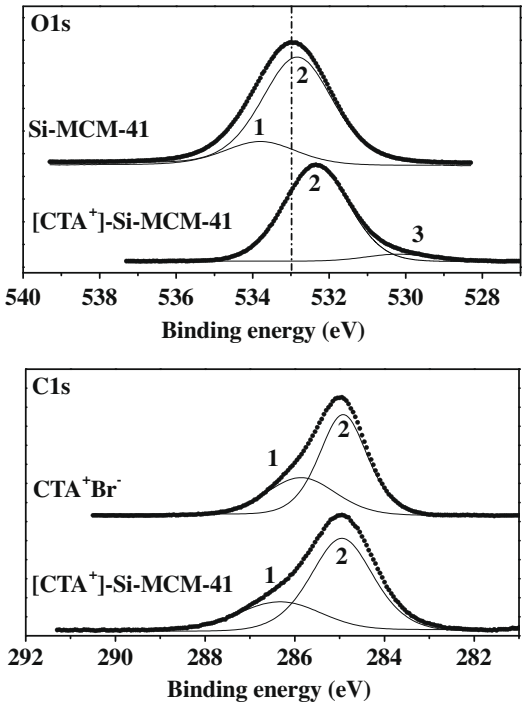

Fig. 4. O1s and C1s XPS spectra of [CTA⁺]–Si–MCM-41, Si–MCM-41 and CTABr.

Table 3
Attribution of decomposed signals observed in XPS spectra.

Signal	O1s		C1s	
	Energy (eV)	Group	Energy (eV)	Group
1	533.8	≡SiOH	286.4–285.9	$(CH_3)_3$–⁺N–C_xH_{2x+1}
2	532.8–532.3	SiO_2	284.9	–C_yH_{2y+1} (alkyl chain)
3	530.2	≡SiO⁻ $(CH_3)_3$–⁺N–	–	–

The existence of the ionic pair ≡SiO⁻CTA⁺ is also supported by the results obtained regarding the chemical composition of the sample. The molar ratio Br/N in CTABr precursor was of 1.1, a number quite close to 1 of the original cationic surfactant. On the other hand, the molar ratio in [CTA⁺]–Si–MCM-41 was found to be 0.08. This is an indication that there is another anion balancing the CTA⁺ cation charge, namely the siloxy anions. The compositional XPS analysis also confirmed the formation of a stoichiometric SiO_2 network containing the CTA⁺ cation. The ascertained C/N ratio of 23 is close to the expected value of 19 of the CTA⁺ cation.

4.2. Catalytic experiments

The Knoevenagel condensation between benzaldehyde and ethyl cyanoacetate was carried out both in the presence (Table 4) as well as in the absence of toluene (Table 5), where 1.9 wt.% of the different siliceous catalysts (A–D) was used in a batch reactor for 3 h. With these catalysts, the reaction resulted in different benzaldehyde conversion to form ethyl-2-cyano-3-phenylacrylate. The widely accepted mechanism in Knoevenagel condensation involves the formation of the anion of ethyl cyanoacetate followed by its attack on the carbonyl group of benzaldehyde. Neither benzyl alcohol nor benzoic acid was observed in the GC-chromatograms of the reaction products, indicating that Cannizzaro reaction does not take place under these experimental conditions. This finding was confirmed by the verification of the selectivity values depicted in Tables 4 and 5, which remained always close to 100%.

The reaction results showed that pure silica resulted in negligible benzaldehyde conversion (<2%) in all cases. In contrast, significant conversions were obtained over the organic–inorganic hybrid catalyst [CTA⁺]–Si–MCM-41. In this case, the catalyst was suggested to have active sites originated from the presence of SiO⁻CTA⁺ ionic pair, and as a result of the weak interaction of the organic cation with the siloxy anion. This catalyst is found to be very attractive, once it can be quite useful in general heterogeneous catalysis, particularly in the synthesis of fine chemicals in apolar media. From Table 4, the catalysts activity can be ordered as follows: [CTA⁺]–Si–MCM-41 > AP–Si–MCM-41 > Cs_2O–Si–MCM-41 > Si–MCM-41. It is important to point out that a literature revision of several solid catalysts used in the Knoevenagel condensation, with benzaldehyde as carbonyl group, revealed that [CTA⁺]–Si–MCM-41 can achieve comparable conversions at much lower temperature (see Supplementary material).

Table 4 shows that the catalyst [CTA⁺]–Si–MCM-41 in the presence of toluene gives higher yields (79.7% after 3 h) in the

Table 4
Effect of the different MCM-41 catalysts A–D on Knoevenagel condensation at 30 °C and 1.9 wt.% of catalyst, using toluene as solvent.

Catalyst		1 h – Toluene		3 h – Toluene	
		Benzaldehyde conversion (%)	Selectivity (%)	Benzaldehyde conversion (%)	Selectivity (%)
A	[CTA⁺]–Si–MCM-41	59.8	98.9	79.7	98.8
B	Si–MCM-41	0	–	2.0	100
C	AP–Si–MCM-41	22.8	100	49.7	100
D	Cs_2O–Si–MCM-41	2.9	100	2.8	100

Table 5
Effect of the different MCM-41 catalysts A–D on Knoevenagel condensation at 30 °C and 1.9 wt.% of catalyst, without solvent.

Catalyst		1 h		3 h	
		Benzaldehyde conversion (%)	Selectivity (%)	Benzaldehyde conversion (%)	Selectivity (%)
A	[CTA$^+$]–Si–MCM-41	40.6	95.4	57.2	99.0
B	Si–MCM-41	0.4	100	0.3	100
C	AP–Si–MCM-41	26.1	99.3	40.3	99.5
D	Cs_2O–Si–MCM-41	32.6	98.3	39.3	99.0

Knoevenagel reaction when compared to solvent-free conditions (57.2% in Table 5). In contrast, the Cs_2O–Si–MCM-41 catalyst showed an opposite behavior, being more active in the absence of toluene. This is probably related to the leaching of cesium as CsOH in polar media. In such a case, the occurrence of homogeneous catalysis is likely to be seen. Regarding the [CTA$^+$]–Si–MCM-41 catalyst, the presence of the solvent possibly dissolves the solid product formed at the pore-mouth, thus increasing the conversion. This could be pointed out as a drawback with regard to the use of [CTA$^+$]–Si–MCM-41 catalyst, since solvent-free conditions are desired in eco-friendly processes. Nevertheless, this catalyst shows an extremely interesting activity in comparison with the AP–Si–MCM-41 and Cs_2O–Si–MCM-41 catalysts, which undergo several treatments and yet present lower activity.

The Knoevenagel reaction of ethyl cyanoacetate (p*K*a = 8.6) is a reaction that can be performed in mild conditions. For this reason, we also conducted the Claisen–Schmidt reaction that is a more demanding reaction by using acetophenone (p*K*a = 15.8), a less acidic organic substance. The Claisen–Schmidt reaction was performed under similar conditions, except the higher temperature (120 °C), because the formation of the acetophenone anion tends to be more difficult owing to the lower acidity of this reactant. Table 6 shows that in this reaction, the catalyst [CTA$^+$]–Si–MCM-41 was also the most active, only 22.8% of benzaldehyde conversion was obtained though.

Also important is the catalyst stability, and therefore we have conducted further experiments in order to test [CTA$^+$]–Si–MCM-41 long-term catalytic activity. Impregnated and functionalized Si–MCM-41 catalysts were already evaluated by other authors. Ernst et al. [21] used Cs_2O–Si–MCM-41 as basic catalyst in Knoevenagel condensation, and they expected some deactivation to occur, since Cs_2O could be hydrolyzed to CsOH. However, no leaching of cesium was observed, and the reason is that reaction was conducted in toluene, *i.e.* in apolar media. Similarly, Jaenicke et al. [26] investigated Si–MCM-41 catalysts with different functionalized organic bases in the formation of monoglycerides from lauric acid. In several reaction cycles, these catalysts demonstrated similar activity after each cycle. In the majority of the cases, improved selectivity was observed. Despite these good performances, they reported that pore volume and surface area of these catalysts were considerably reduced after the first cycle [26].

Table 6
Effect of the different MCM-41 catalysts A–D on Claisen–Schmidt condensation at 120 °C and 1.9 wt.% of catalyst, without solvent.

Catalyst		Benzaldehyde conversion (%)	Selectivity (%)
A	[CTA$^+$]–Si–MCM-41	22.8	96.4
B	Si–MCM-41	0.7	100
C	AP–Si–MCM-41	14.4	99.0
D	Cs_2O–Si–MCM-41	1.1	95.2

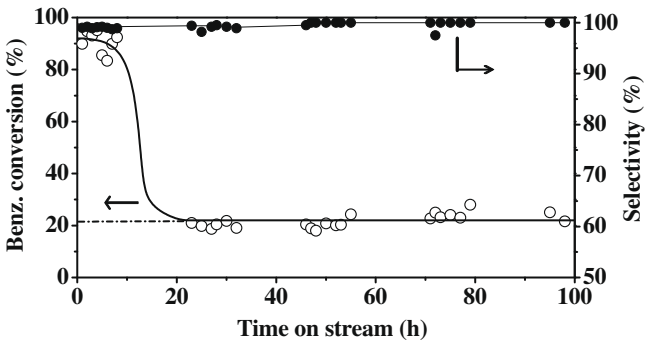

Fig. 5. Benzaldehyde conversion over pelletized [CTA$^+$]–Si–MCM-41 catalyst at 30 °C and up to 100 h on stream (benzaldehyde and ethyl cyanoacetate mixture in toluene).

In order to verify the long-term catalytic stability of [CTA$^+$]–Si–MCM-41, this catalyst was pressed into pellets and tested in a continuous flow reactor up to 100 h at 30 °C. The results are shown in Fig. 5. A very strong initial deactivation was detected. However, no further deactivation was observed, and benzaldehyde conversion was kept always around 22%. The deactivation is attributed to the leaching of CTA$^+$ cations that are weakly connected to the micelles in the [CTA$^+$]–Si–MCM-41 catalyst [9]. After that the activity maintains, as the residual CTA cations (strongly connected to micelles) did not leach anymore. Thermogravimetric measurements revealed that after 100 h of reaction, CTA$^+$ cation quantity was reduced from *ca.* 38 wt.% to 32 wt.%.

In a previous work [10], we checked whether homogeneous catalysis was responsible for the high activity of the [CTA$^+$]–Si–MCM-41 catalyst. This was done by removing the catalyst from the reaction mixture through centrifugation, and the composition of the remaining liquid was then monitored, and no reaction was further observed. Thus, the development of homogeneous catalysis by any leached species was excluded.

5. Conclusions

As-synthesized [CTA$^+$]–Si–MCM-41 catalyst exhibited higher activity in Knoevenagel and Claisen–Schmidt condensation reactions than the modified AP–Si–MCM-41 and Cs_2O–Si–MCM-41 molecular sieves. Calcined Si–MCM-41 showed negligible activity, as it contains no catalytic centers. The active sites in [CTA$^+$]–Si–MCM-41 are related to siloxy anions, which are combined with bulky CTA cations. Partial leaching of these organic cations was observed in the beginning of time on stream as demonstrated in the continuous flow experiment. However, as this catalyst still shows high activity, reactions can be conducted at low temperatures, and under these conditions, they show long-term stability. In general, this catalyst might be useful for basic heterogeneous catalysis, particularly for the synthesis of fine chemicals via an eco-friendly route.

Acknowledgments

The authors wish to thank DAAD/Germany (Deutscher Akademischer Austausch Dienst) and CNPq/Brazil (Conselho Nacional de

Desenvolvimento Científico e Tecnológico) for awarding a PhD grant to Leandro Martins.

Appendix A. Supplementary material

Supplementary data associated with this article can be found, in the online version, at doi:10.1016/j.jcat.2010.01.015.

References

[1] H. Hattori, Chem. Rev. 95 (1995) 537.
[2] K. Tanabe, W.F. Hölderich, Appl. Catal. A: Gen. 181 (1999) 399.
[3] M.H. Valkenberg, W.F. Hoelderich, Catal. Rev. 44 (2002) 321.
[4] L. Martins, D. Cardoso, Quim. Nova 29 (2006) 358.
[5] J.S. Beck, J.C. Vartuli, W.J. Roth, M.E. Leonowicz, C.T. Kresge, K.D. Schmitt, C.T.W. Chu, D.H. Olson, E.W. Sheppard, S.B. McCullen, J.B. Higgins, J.L. Schlenker, J. Am. Chem. Soc. 114 (1992) 10834.
[6] F. Fajula, D. Brunel, Micropor. Mesopor. Mater. 48 (2001) 119.
[7] Y. Kubota, Y. Nishizaki, H. Ikeya, J. Nagaya, Y. Sugi, in: A. Sayari, M. Jaroniec (Eds.), Nanoporous Materials III, Studies in Surface Science and Catalysis, vol. 141, Elsevier, Amsterdam, 2002, p. 553.
[8] Y. Kubota, Y. Nishizaki, H. Ikeya, M. Saeki, T. Hida, S. Kawazu, M. Yoshida, H. Fujii, Y. Sugi, Micropor. Mesopor. Mater. 70 (2004) 135.
[9] L. Martins, T.J. Bonagamba, E.R. Azevedo, P. Bargiela, D. Cardoso, Appl. Catal. A: Gen. 312 (2006) 77.
[10] L. Martins, D. Cardoso, Micropor. Mesopor. Mater. 106 (2007) 8.
[11] L. Martins, D. Cardoso, in: D. Zhao, S. Qiu, Y. Tang, C. Yu (Eds.), Recent Progress in Mesostructured Materials, Studies in Surface Science and Catalysis, vol. 165, Elsevier, Amsterdam, 2007, p. 761.
[12] Y. Kubota, H. Ikeya, Y. Sugi, T. Yamada, T. Tatsumi, J. Mol. Catal. A: Chem. 249 (2006) 181.
[13] R. Srivastava, D. Srinivas, P. Ratnasamy, Tetrahedron Lett. 47 (2006) 4213.
[14] N. Baccile, G. Laurent, C. Bonhomme, P. Innocenzi, F. Babonneau, Chem. Mater. 19 (2007) 1343.
[15] A.A. Romero, M.D. Alba, W. Zhou, J. Klinowski, J. Phys. Chem. B 101 (1997) 5294.
[16] S. Hitz, R. Prins, J. Catal. 168 (1997) 194.
[17] Z.H. Li, S.J. Roy, Y.Q. Zou, R.S. Bowman, Environ. Sci. Technol. 32 (1998) 2628.
[18] R. Pool, P.G. Bolhuis, J. Phys. Chem. B. 109 (2005) 6650.
[19] X. Wang, Y.-H. Tseng, J. C.C. Chan, S. Cheng, J. Catal. 233 (2005) 266.
[20] C.N. Pérez, E. Moreno, C.A. Henriques, S. Valange, Z. Gabelica, J.L.F. Monteiro, Micropor. Mesopor. Mater. 41 (2000) 137.
[21] S. Ernst, T. Bongers, C. Casel, S. Munsch, in: I. Kiricsi, G. Pál-Borbély, J.B. Nagy, H.G. Karge (Eds.), Porous Materials in Environmentally Friendly Processes, Studies in Surface Science and Catalysis, vol. 125, Elsevier, Amsterdam, 1999, p. 367.
[22] V.K. Díez, C.R. Apesteguía, J.I. Di Cosimo, J. Catal. 240 (2006) 235.
[23] S. Brunauer, P.H. Emmet, E. Teller, J. Am. Chem. Soc. 60 (1938) 309.
[24] M. Kruk, M. Jaroniec, Langmuir 13 (1997) 6267.
[25] K.R. Kloetstra, M. van Laren, H. van Bekkum, J. Chem. Soc. Faraday Trans. 93 (1997) 1211.
[26] S. Jaenicke, G.K. Chuah, X.H. Lin, X.C. Hu, Micropor. Mesopor. Mater. 35–36 (2000) 143.